Nuclear Instruments and Methods in Physics Research B 268 (2010) 414–419

Contents lists available at ScienceDirect

Nuclear Instruments and Methods in Physics Research B

journal homepage: www.elsevier.com/locate/nimb

A thin film approach to protein crystallography

M. Birkholz

IHP, Im Technologiepark 25, 15236 Frankfurt (Oder), Germany

ARTICLE INFO

Article history:
Received 2 June 2009
Received in revised form 18 August 2009
Available online 7 October 2009

Keywords:
Macromolecular crystallography
Thin films
Nanotemplates
Grazing incidence X-ray diffraction (GIXRD)
Laue diffraction

ABSTRACT

A novel approach for the investigation of proteins or macromolecules is outlined in this conceptual study. The preparation of grapho-epitaxial layers on nanotemplated substrates is proposed as an alternative to the preparation of single crystals by vapour diffusion techniques. Crystal structure investigations of such layers may then be performed via grazing-incidence diffraction (GIXRD) in the Laue mode. Quantitative expressions for the position and intensities of XRD peaks in this geometry are presented that fully consider the effects of refraction and absorption. A simulation of the Laue-GIXRD pattern of single-crystalline layers of Concanavalin A is given. The main challenges of the approach are concluded to relate to the preparation of single-crystalline protein layers. However, if those obstacles could be overcome, a 10–100-fold faster sample throughput would become possible.

1. Introduction

X-ray diffraction (XRD) still is the essential characterization technique to elucidate the three dimensional structure of proteins. Although the required crystallization constrains the protein into an artificial association, in which it never occurs under natural conditions, XRD supplies the decisive structural information for understanding the molecular function. It might be hoped that someday bio-informatics will allow the prediction of a protein 3D structure from the sequence of amino acids. Although remarkable steps were taken in this direction [1], macromolecular crystallography still faces the task of preparing single crystals, which represents the rate-determining step for the structure solution as requested by biophysics and the life sciences in general [2].

In this work, a concept will be outlined how functionalized surfaces may be applied to the preparation of thin protein films or, in general, macromolecular films and their subsequent structural investigation by X-ray diffraction. The technology of thin films has become an important branch of materials science [3] and a large set of experimental knowledge has been gathered describing thin film growth, morphology and structure [4]. These many experiences justify to seriously elucidate the perspectives of thin macromolecular films as a complement to single crystals. It will be argued here that the numerous nanotemplating methods available in nowadays semiconductor technology allow for the preparation of well adopted substrates for the locally controlled immobilization of protein molecules, monolayers and fully crystalline layers. The approach is motivated by the fact that recent minimum feature dimensions in the fabrication of semiconductor circuits have entered the sub-100 nm range [5] and have thus arrived on the order of spatial dimensions of large biological molecules.

In the first part of the paper, the major aspects in XRD of single protein crystals and perspective thin films will be compared. Also, the challenges in the preparation of such layers will be considered. The main part will outline how the GIXRD technique (grazing-incidence X-ray diffraction) in a multiple wavelength Laue mode may be modified for the collection of a sufficiently large set of Bragg peaks from macromolecular layers. The concept will be illustrated by simulating the diffraction pattern of concanavalin A (ConA), a 26 kDa protein from the group of lectins the structure of which has been thoroughly worked out [6–8] and which is considered for biomedical applications in a continuously operating glucose sensor [9].

2. The basic approach

The optimum sample volume in a scattering experiment is determined by the linear attenuation coefficient μ of the radiation and should attain values on the order of $V_{sc} \approx 1/\mu^3$. This choice assures the interaction of radiation with the sample to become both sufficiently large, to induce a strong enough scattering, and sufficiently weak, to reach the detector. The density of protein crystals ranges from 1.22 to 1.47 g cm^{-3} [10,11], while their elemental composition can be approximated by the chemical formula C_4NO. The latter derives from averaging over all naturally occurring amino acids in their polymerized form, if low-scattering hydrogen atoms and low-concentrated components like sulphur and metals are neglected. Inserting the elemental mass absorption

E-mail address: birkholz@ihp-microelectronics.com

0168-583X/$ - see front matter © 2009 Elsevier B.V. All rights reserved.
doi:10.1016/j.nimb.2009.09.054

coefficients [12] and an average density of 1.35 g cm^{-3}, the linear attenuation coefficient μ of protein crystals is calculated to lie between 21 and 0.62 cm^{-1} for standard X-ray wavelengths from 6 to 20 keV. Accordingly, the specimens' extension in protein XRD crystallography would advantageously amount from 0.5 to 16 mm. Although crystals with edges in excess of 1 mm are rarely prepared, samples of some 100 μm are routinely measured. These values also fit well to the widely used Cu Kα line (8 keV, $\mu = 12$ cm^{-1}) and to typical diameters of collimated X-ray beams. Even smaller crystals with volumes on the order of (50 μm)^3 became measurable by the introduction of microdiffraction [13] and the usage of highly brilliant synchrotron radiation. Altogether, the volume of specimens investigated in protein crystallography roughly obeys the golden rule of single-crystal diffraction, $V_{sc} \approx 1/\mu^3$.

Scattering volumes of about (100 μm)^3, however, are not only delivered by single crystals exhibiting the same extension in every spatial direction. Rather, thin single-crystalline layers with lateral edges elongated at the expense of vertical height may also apply. For instance, a flat protein slab with a thickness of 1 μm and lateral edges of 5 × 0.2 mm would equally yield the required scattering volume of $1/\mu^3$. This sample geometry points to the field of thin film technology, where single-crystalline layers of appropriate vertical extension are routinely been dealt with.

A decisive advantage of the thin film approach will be related to its probably much higher process velocity. The growth of protein crystals takes days to weeks for the commonly used vapour diffusion techniques in order to arrive at scattering objects of appropriate dimensions [2]. This is essentially due to the low energy of cohesion between molecules in a protein crystal and the small growth velocity v on the order of μm/h. In case of a thin film, however, the decisive process would be the vertical growth, since the layer growth would start and proceed simultaneously on all covered areas of the substrate. Assuming that the film growth rate R would be on the same order of magnitude as for bulk crystal specimen, $R \approx v$, the preparation of a 1 μm thin layer would take only a time span of about an hour. The sample preparation would thus be associated with an acceleration factor of 10–100 compared to single crystal preparation techniques. The thin film approach thus appears very promising from the point of view of high sample throughput and the question arises: what has been done so far to arrive at such interesting sample material?

Remarkably, already in 1988 McPherson and Shlichta demonstrated hetero-epitaxy of proteins on a solid support. In their case the growth of a layer of hen-egg white lysozyme on apophyllite was likely to be truly epitaxial as shown by X-ray diffraction [14]. However, this special case was apparently only one out of 200 combinations from 50 minerals with four proteins that all failed – except one – with respect to hetero-epitaxy. It seems that no further examples of epitaxial growth of proteins on other single crystals have been reported in the literature. The most widely used technique for biomolecular immobilization is due to covalent bonding with crosslinking molecules like the covering of SiO_2 surfaces with silanes [15–17]. Complete 3D architectures of protein layers have been constructed on the basis of such immobilized monolayers reaching up to a height of some dozen molecules, but the technique failed in the preparation of 3D crystalline specimens [18].

An alternative route may be taken by the usage of graphoepitaxy [3], where a template is inscribed into the substrate surface with a lateral periodicity or pitch p that is a multiple of the lattice parameter of the epitaxial layer. For an orthorhombic crystal with cell parameters a, b and c and an intended growth direction along c, for instance, $p_x = na$ and $p_y = mb$ should hold (n and m integers). This choice should assure that the different grains starting to grow at different positions on the substrate will merge into one large crystal when their lateral growth causes them to coalesce. Various nanostructuring techniques allow for the preparation of such templates having pitches p on the order of some 100 nm, among them the highly developed semiconductor technology. The potentials of the latter encompass the preparation of Si-based nanotemplates by use of a buried dislocation array [19] or of surface doping lattices by patterning of wafer surfaces [20].

Graphoepitaxy has successfully been demonstrated by Givargizov et al. for the growth of small single crystals of catalase and concanavalin A [21], where use was made of micropatterned arrays on oxidized silicon wafers exhibiting pitches of 10 and 15 μm. However, only unconnected crystals were grown, while a complete homogeneous coverage of the substrate by a thin protein film was not in the focus of the study and remained unobtained. The conclusions could be drawn from this work that smaller pitches of surface templates in the sub-μm range should be used. There is good reason to assume that the preparational bottle neck identified by Givargizov et al. might be circumvented by using the modern techniques for surface nanostructuring and that such single-crystalline layer will become available in the near future. It will thus be developed and elucidated the XRD formalism for the structural investigations of such samples in the remaining part of this work.

3. The diffraction pattern

Grapho-epitaxial layers of crystalline macromolecules would have to be measured by X-ray diffraction in a reflection configuration as sketched in Fig. 1. Scattered reflections would be observed on an area detector placed at a distance R_0 from the centre of the layer. The incoming X-ray beam must impinge onto the sample surface under a very small incidence angle α on the order of 1°, in order to excite scattering in the full sample volume. For the measurement of a sufficiently large set of Bragg reflections, polychromatic X-rays have to be applied as in a Laue experiment. XRD in the Laue mode has become a valuable tool in protein crystallography, in particular with respect to time-resolved studies [22,23]. Measurements for the purpose of this work will thus have to be performed at synchrotron beam lines that allow for the irradiation with a full X-ray spectrum. In case of protein crystals, the used energy band may be restricted to $6 \leqslant E \leqslant 20$ keV, because radiation damage becomes too severe for lower energies and the scattering cross section diminishes strongly for higher ones.

Orthorhombic crystals will be considered as examples in the following, which is justified by the fact that the majority of protein crystals occur in orthorhombic and tetragonal space groups [10]. For reasons of simplicity, the spectrum of the incident radiation will be assumed to attain the shape of a box function, having $I(\lambda) = 0$ for wavelengths $\lambda < \lambda_{min}$ or $\lambda > \lambda_{max}$ and $I = I_0$ otherwise. An additional simplification is introduced by assuming the crystal reference frame $\{\boldsymbol{c_i}\} = \{a, b, c\}$ to coincide with the sample reference frame $\{\boldsymbol{s_i}\}$ having $a \| -\boldsymbol{s}_1$, $b \| \boldsymbol{s}_2$ and $c \| \boldsymbol{s}_3$. If the incidence angle is set to the constant value α, the positions of reflections in space are accounted for by the exit angle β and azimuth ϕ, see Fig. 1. The Laue equations $\boldsymbol{Q} = \boldsymbol{K} - \boldsymbol{K}_0 = 2\pi \mathrm{g}_{hkl}$ of this experiment then read

$$\begin{aligned} \cos\beta\cos\phi - \cos\alpha &= -h\lambda/a \\ \cos\beta\sin\phi &= k\lambda/b \\ \sin\beta + \sin\alpha &= l\lambda/c \end{aligned} \tag{1}$$

which can be regarded as a system of three equations for the three unknowns λ, β and ϕ of any reflection hkl to occur.

The incidence angle α has to exceed the critical angle α_c, below which the incoming X-ray beam would be totally reflected. The

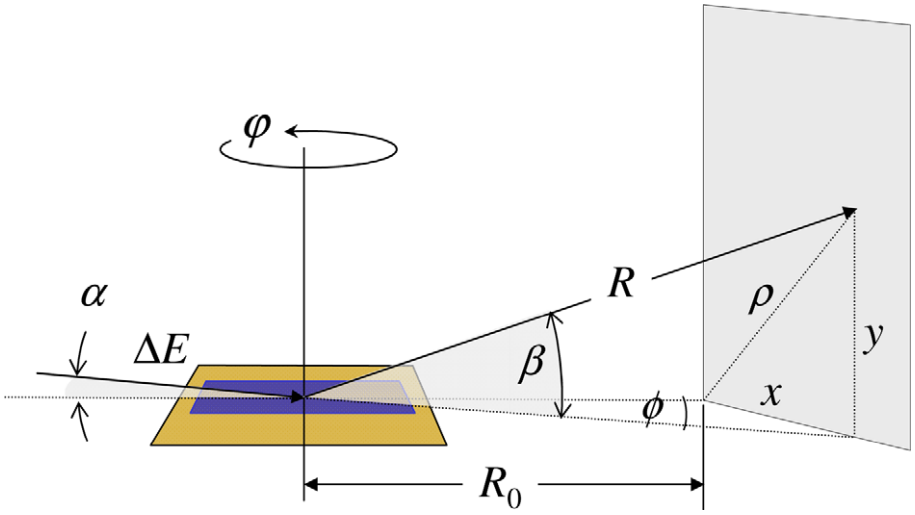

Fig. 1. Experimental set-up proposed in this work for XRD investigations of thin protein layers. As in grazing-incidence diffraction (GIXRD) the incoming beam impinges on the sample under a small incidence angle α. In contrast to GIXRD, the beam encompasses a complete band of X-rays of different energies and probes the volume of the layer. Scattered beams are mapped on a flat area detector at a distance R_0 from the layer's centre of gravity. Detector coordinates of individual Bragg peaks are denoted by x, y and ρ. The sample may be set to other spindle angles φ in order to scan different parts of reciprocal space.

critical angle α_c derives from the complex refractive index $n = 1 - \delta - i\mu\lambda/4\pi$ that is usually represented by small deviations δ and $\mu\lambda/4\pi$ from unity (the symbol β is often used to indicate the imaginary part of n, which is avoided here, since β stands for the exit angle of the diffracted radiation). According to Snell's law the critical angle is related via $\alpha_c = \arccos(1\text{-}\delta\text{-}i\mu\lambda/4\pi)$ to the material constants δ and μ, but for the case of small absorption $\mu\lambda/4\pi \ll \delta$, the approximation $\alpha_c = \sqrt{2\delta}$ yields reliable results. Numerical values of α_c range between 0.3° and 0.07° in the relevant energy range for the model compound C_4NO of 1.35 g/cm^3 density. By choosing an incidence angle of about 1° one would thus safely operate above α_c for all beam energies.

The system of Eqs. (1) is an oversimplification in so far as it leaves the refraction of X-rays unconsidered. Adjusting the incidence angle to values on the order of 1°, however, the effect should be taken into account, since it will cause a shift of reflections to higher exit angles β. If one considers a certain reflection hkl to appear on the detector, the respective X-ray beam has been subjected twice to refraction: once while entering the layer and secondly on exiting from it. Accordingly, only the incidence angle α and the exit angle β are affected, while the azimuth ϕ remains unchanged. The effect is visualized in Fig. 2 for a reflection $h0l$ having $\phi = 0$. It is realized from the figure that the incidence angle of the transmitted wave α_t and the exit angle of the scattered wave β_s are the appropriate quantities to be inserted in the Laue equations. These differ from both angles to be observed outside the sample α and β, and the difference increases the smaller both angles becomes. The discrepancy can be resolved by applying Snell's law again, that yields for refraction on the incidence side

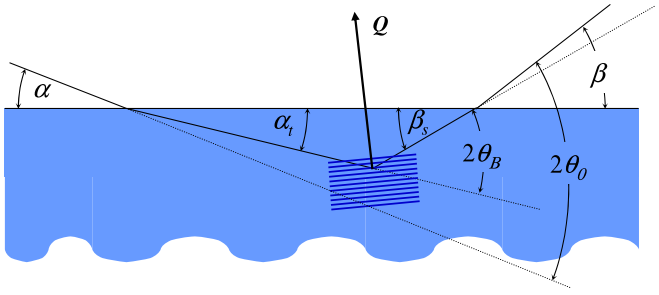

Fig. 2. Schematic representation of the effect of refraction for incoming and exiting X-ray beam.

$$\alpha_t = \arccos\frac{\cos\alpha}{1-\delta-i\mu\lambda/4\pi} \tag{2}$$

This complex number $\alpha_t = \mathrm{Re}(\alpha_t) + i\mathrm{Im}(\alpha_t)$ may be rewritten as

$$\alpha_t = \arccos(A_t^+ - A_t^-) - i\ln(A_t^+ + A_t^- + \sqrt{(A_t^+ + A_t^-)^2 - 1}) \tag{3}$$

with the abbreviations having the meaning

$$A_t^{\pm} = \frac{1}{2}\sqrt{\left(\frac{(1-\delta)\cos\alpha}{(1-\delta)^2 + (\mu\lambda/4\pi)^2} \pm 1\right)^2 + \frac{(\mu\lambda/4\pi)^2\cos^2\alpha}{((1-\delta)^2 + (\mu\lambda/4\pi)^2)^2}} \tag{4}$$

The angle of the transmitted wave α_t thus consists of purely real and imaginary components accounting for the effects of refraction and absorption, respectively. Comparable expressions are valid for β_s, where angle α and index t have to be replaced by β and s

$$\beta_s = \arccos(B_s^+ - B_s^-) - i\ln(B_s^+ + B_s^- + \sqrt{(B_s^+ + B_s^-)^2 - 1})$$
$$B_s^{\pm} = \frac{1}{2}\sqrt{\left(\frac{(1-\delta)\cos\beta}{(1-\delta)^2 + (\mu\lambda/4\pi)^2} \pm 1\right)^2 + \frac{(\mu\lambda/4\pi)^2\cos^2\beta}{((1-\delta)^2 + (\mu\lambda/4\pi)^2)^2}} \tag{5}$$

In fact, the shift of reflections is small, but for a quantitative evaluation of lattice parameters, it has to be taken into account. The correction may be applied by usage of α_t and β_s instead of α and β in Eq. (1), which results in the new system of Laue equations

$$\begin{aligned}(B_s^+ - B_s^-)\cos\phi - (A_t^+ - A_t^-) &= -h\lambda/a\\ (B_s^+ - B_s^-)\sin\phi &= k\lambda/b\\ \sqrt{1-(B_s^+ - B_s^-)^2} + \sqrt{1-(A_t^+ - A_t^-)^2} &= l\lambda/c\end{aligned} \tag{6}$$

relating the scattering parameter λ, ϕ and β to lattice parameters a, b, c and material constants δ and μ.

A decisive quantity for the experimental set-up proposed here is the average information depth $\bar{\tau}$, from which the structural infor-

mation derives [4]. This quantity is calculated from the weighted sum over all depths z contributing to scattering

$$\bar{\tau} = \frac{\int_0^t z \exp(-Mz) dz}{\int_0^t \exp(-Mz) dz} \tag{7}$$

with integrals limited by the layer thickness t. For small incidence and exit angles the damping factor M may not simply be described by $2\mu/\sin\theta$ (as appropriate for a $\theta/2\theta$ scan), but the analysis of a plane electromagnetic wave traversing a phase boundary shows that the damping of intensity is governed by the imaginary part of the product of refractive index and the sine of the transmitted wave [4]. Inserting the sine of α_t and β_s as appropriate for the case considered here, one ends up with the result

$$M = -\frac{4\pi}{\lambda}(\mathrm{Im}(n\sin\alpha_t) + \mathrm{Im}(n\sin\beta_s)) \tag{8}$$

The minus sign on the rhs is required in case of the usual notation of $n = 1 - \delta - i\mu\lambda/4\pi$. The integral is solved to yield

$$\bar{\tau} = t\left(\frac{1}{Mt} + \frac{1}{1-\exp(Mt)}\right) \tag{9}$$

The course of $\bar{\tau}/t$ for C_4NO as a function of energy is displayed in Fig. 3, which shows monotonic behaviour, since no X-ray absorption edges of C, N or O occur in the energy range of interest. It is realized from the plot that a setting of $\alpha = 1°$ would be a reliable choice for an intended information depth of a few 100 nm for a 1 μm thin film.

Regarding the integral intensity I_{hkl} of a Bragg peak from a single-crystalline protein layer, the use of kinematical diffraction theory appears reliable due to the low-Z composition and the large unit cells of protein crystals. I_{hkl} then depends on the square of the structure factor $|F_{hkl}|^2$, the Lorentz-polarization factor Lp, the sample to point-of-detection distance R and an instrumental scaling factor SCF. For polychromatic exposure and a stationary specimen, it may be written

$$I_{hkl} = \int SCF\, R^{-2}\, \lambda^2\, Lp\, |F_{hkl}|^2\, I\, dV \tag{10}$$

with the integration to be performed over the full scattering volume [24]. The Lorentz factor in single-crystal diffraction is $1/\sin 2\theta$, while the polarization of the incident radiation may be assumed in synchrotron experiments to exhibit a dominant component in the y-direction yielding a $\cos^2\phi$ polarization for the scattered beam and $Lp = \cos^2\phi\ /\sin 2\theta$ finally results. For homogeneous single-crystalline layers, most factors in the integral kernel become independent of where the scattering occurs and can be placed before the integral.

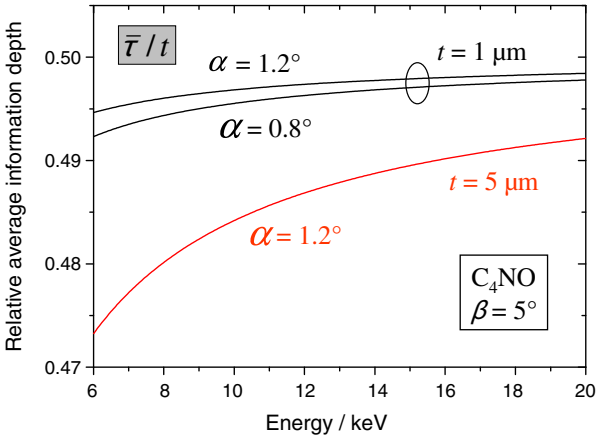

Fig. 3. Relative average information depth $\bar{\tau}/t$ for an exit angle β of 5°. Parameters indicate different incidence angles and layer thickness.

The incoming intensity I_0, however, is attenuated during its passage through the sample and thus becomes a function of sample depth z. Rewriting the infinitesimal volume as $dV = Sdz/\sin\alpha_t$, with S being the incident beam area, the integral intensity becomes

$$I_{hkl} = SCF\, R^{-2}\, \lambda^2\, Lp\, |F_{hkl}|^2\, \frac{S}{\sin\alpha_t} \int_0^t I(z)\, dz \tag{11}$$

The depth variation may again be described by the M factor introduced in Eq. (8) and we may express the integral intensity by

$$I_{hkl} = SCF\, R^{-2}\, \lambda^2\, Lp\, |F_{hkl}|^2\, \frac{S}{\sin\alpha_t} I_0 \frac{1}{M}(1 - \exp(-Mt)) \tag{12}$$

Introducing the absorption factor $A(t) = 1 - \exp(-Mt)$ [4] and lumping the beam area S into SCF one finally ends up with the equation

$$I_{hkl} = SCF\, I_0\, R^{-2}\, \lambda^2\, Lp\, |F_{hkl}|^2\, \frac{1}{M\sin\alpha_t} A(t) \tag{13}$$

This equation represents the final expressions for the integral intensities of Bragg reflections scattered from a single-crystalline layer in a grazing-incidence configuration under full consideration of refraction and absorption.

Among other factors, the applicability of the thin film approach will depend on the divergence of the scattered reflections and a sufficient separation of Bragg peaks on the detector screen. The divergence w will be determined by (i) the divergence of the incoming beam, (ii) the geometry of scattering and (iii) sample properties, mainly the mosaic spread of single-crystalline domains in the macromolecular layer. The first factor may be reduced to very small values when operating the experiment at a synchrotron beam line. The third factor is difficult to estimate on the current state of knowledge, but the second factor can be estimated from geometrical considerations. A close inspection of Fig. 1 reveals the geometrical divergences in x and y direction to scale with $w_y = L\sin\beta$ and $w_x = L\sin\phi$, when L is the irradiated length of the sample. For a 200 × 200 mm detector at a distance of $R = 500$ mm, a sample length of $L = 5$ mm would thus induce extensions of X-ray peaks maximally on the order of 2 mm. In general, the geometry-related divergence in this experimental configuration will remain small, since it operates in a nearly forward scattering mode due to the large lattice parameters. Factor (i) and (ii) thus would not prevent the application of the approach proposed here.

Concanavalin A from *Canavalia ensiformis* served as an example for testing the approach. ConA crystallizes in an orthorhombic unit cell $P2_12_12_1$ or $I222$, depending on bonded glucoligands, steric interactions of monomers and crystallization conditions [7]. A computer program GILaue [25] was developed to simulate the diffraction pattern from a ConA layer in the assumed configuration as shown in Fig. 2. Eq. (6) was solved by setting the incidence angle $\alpha = 1°$, and cell parameters a, b and c of 6.32, 8.74 and 8.93 nm were inserted according to PDB structure 1DQ6 [7]. The final result is shown in Fig. 4, where the calculated positions of reflections and their integral intensity on a 200 × 200 mm detector screen are given for R_0 amounting to 500 mm and X-ray energies confined to 6–20 keV. Individual peak profiles were modelled to be of Cauchy/Lorentz type to sum up to the complete pattern via

$$I(x,y) = \sum_{hkl} \frac{I_{hkl}}{(1 + (x - x_{0,hkl})^2/w_x^2 + (y - y_{0,hkl})^2/w_y^2)} \tag{14}$$

with the sum running over all reflections hkl to be observed, when the experimental resolution d_{min} is set to 0.25 nm^{-1}. Divergences w were assumed to be composed of a small instrumental contribution $w_0 = 0.2$ mm (as easily possible for most diffraction set-ups at synchrotrons) and the geometrical terms w_x and w_y given above. The

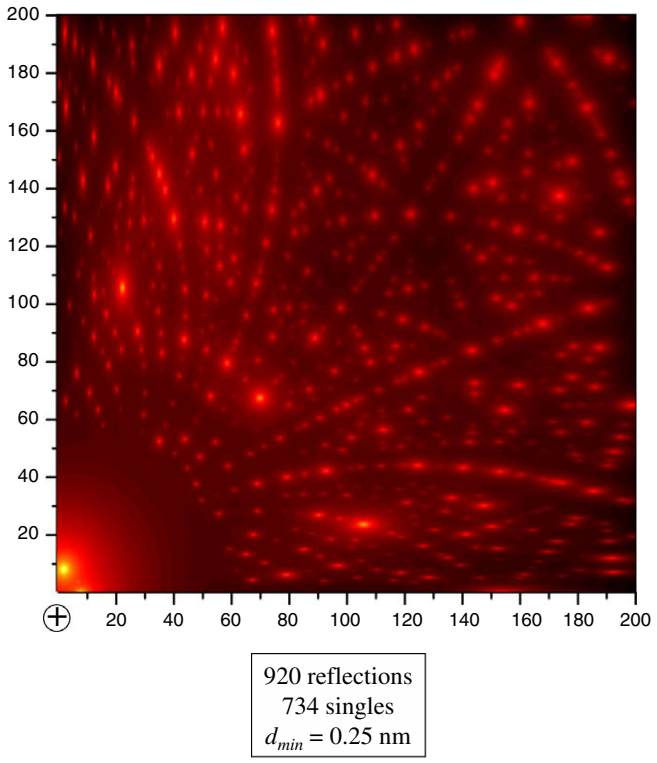

Fig. 4. Simulated Laue reflection pattern of a 1 μm thin epitaxial concanavalin A layer irradiated by white X-rays from 6 to 20 keV. Intensities are given on a logarithmic scale calculated according to Eq. (13).

constants *SCF* and I_0 were set to unity. Squares of the structure factor $|F_{hkl}|^2$ were calculated by inserting the atomic positions as specified by the PDB file 1DQ6 and atomic scattering factors *f* of C, N and O (as though as 2 S and 2 Mn atoms per molecule). The simulated pattern in Fig. 4 shows the typical Laue pattern characteristics with families of reflections lying on conic sections through reciprocal space.

More than 900 reflections would then occur in the experiment, with 734 single reflections, while the other are double reflections and higher harmonics. Next to the peaks displayed in the figure a further high intensity reflection would arise in this experimental configuration that is caused by the specular reflection of the incident beam and that has not been included in the simulation. In a recent GID/GISAXS study on thin films of bacteriorhopsin, i.e. purple membrane patches on Si wafers [26] we showed that only a small part of the detector is affected by the specular reflection and that the majority of diffraction peaks remained analyzable in the scattering configuration sketched in Fig. 1.

4. Discussion and conclusion

It can be concluded that the availability of grapho-epitaxial thin films would enable the determination of a large set of reflection positions and intensities. At the current state of knowledge, it is difficult to give an estimation of the spatial resolution to be obtained with the technique. In conventional protein crystallography the part of reciprocal space to be mapped typically reaches down to resolutions of 0.2–0.5 nm^{-1}, in the full range of which the intensities of some 10^4–10^5 peaks are measured. For the example given above, azimuthal and exit angle ranges amounted to about 22° yielding some 900 reflections. By rotating the sample around the spindle angle φ further positions would contribute to an estimated total of about 15,000 reflections. This number may further be enlarged by tilting and positioning the detector plate to higher polar positions. For too large exit angles β, however, reflections will not be well resolved, since the divergence of the beam scales with $L\sin\beta$, causing an increased broadening and probably too severe peak overlap for increasing β. The collection of additional reflections *hkl* might then become only possible by reducing the sample length *L*, i.e. at the expense of reflection intensity. Further extensions of the number of measurable reflections would become possible with the usage of single-crystalline layers of different crystallographic orientation. Conceptually, such a perspective could be approached by using nanotemplated substrates with surface structures and pitches *p* adapted to the crystallographic characteristics of differently oriented layers. Altogether, the presented measurement is concluded to principally allow the collection of the required number of Bragg reflections to investigate the structure of proteins to a resolution that compares to bulk single crystal studies.

The most significant part of work for establishing the method will be related to the development of successful preparation techniques for grapho-epitaxial protein layers. In this respect, possible drawbacks of the approach should be considered. Firstly, proteins are frequently observed to denaturize when approaching an inorganic surface from solution. Evidently, the complete denaturisation of the bottom-most layer in an intended single-crystalline protein film would severely complicate the subsequent crystal growth. Secondly, proteins have been observed to adapt a different three dimensional structure when adsorbing to a solid support compared with that attained in a bulk solid crystal. The obtained crystal structure then differs from the latter. Both effects have to be taken into account, but at the current state of knowledge it is difficult to decide whether they will turn out as fundamental obstacles to the preparation of single-crystalline layers and it can just be concluded that more experiments are required to extend our spare experimental data base.

To summarize, a novel approach to protein crystallography has been proposed in this work. It has been argued that instead of the commonly used single crystals, the preparation of grapho-epitaxial layers of proteins on nanotemplated substrates might represent a reliable complement or alternative. Such sample material may be analyzed by the established crystallographic techniques as applied to their single crystal counterparts. This work has shown how the GIXRD technique has to be adopted for this purpose and quantitative expressions for the position and intensity of Bragg reflections were given. In order to measure a large number of XRD peaks polychromatic radiation as in the Laue technique must be applied and investigations thus have to be performed at synchrotron beam lines. The diffraction pattern from a single-crystalline Con A layer has been simulated in the given framework demonstrating that the approach would allow the collection of a sufficiently large number of Bragg peaks to solve for the protein structure. The major advantage of the new ansatz is due to the perspective time savings being so significant that they will probably become the decisive argument to firmly pursue the approach.

Acknowledgements

The support of and helpful discussions with C. Genzel, A. Giussani, M. Heyn, M. Kittler, I. Wallat and P. Zaumseil are gratefully acknowledged. This work has partially been funded by the Volkswagen-Stiftung through the SOBSI project.

References

[1] B. Qian, S. Raman, R. Das, P. Bradley, A.J. McCoy, R.J. Read, D. Baker, Nature 450 (2007) 259.
[2] J. Drenth, Principles of Protein X-ray Crystallography, Springer, Berlin, 1999.
[3] M. Ohring, Materials Science of Thin Films: Deposition and Structure, Academic Press, San Diego, 2002.

[4] M. Birkholz, with contributions by P.F. Fewster and C. Genzel, Thin Film Analysis by X-ray Scattering, Wiley-VCH, Weinheim, 2006 (Chapter 4).
[5] International Technology Roadmap for Semiconductors – 2008 Update – Executive Summary. <http://www.itrs.net/Links/2008ITRS/Home2008.htm>.
[6] V. Mikol, R. Giegé, J. Cryst. Growth 97 (1989) 324.
[7] J. Bouckaert, Y. Dewallef, F. Poortmans, L. Wyns, R. Loris, J. Biol. Chem. 275 (2000) 19778.
[8] M.P. Blakeley, A.J. Kalb (Gilboa), J.R. Helliwell, D.A.A. Myles, PNAS 101 (2004) 16405.
[9] M. Birkholz, K.-E. Ehwald, R. Ehwald, M. Kaynak, J. Borngräber, J. Drews, U. Haak, J. Klatt, E. Matthus, G. Schoof, K. Schulz, B. Tillack, W. Winkler, D. Wolansky, in: H. Seidel, H. Reichl, W. Lang (Eds.), Proceedings Mikrosystemtechnik Kongress 2009, Berlin, VDE-Verlag, Berlin, 2009, p. 124.
[10] K.M. Andersson, S. Hovmöller, Acta Crystallogr. D 56 (2000) 789.
[11] M.L. Quillin, B.W. Matthews, Acta Crystallogr. D 56 (2000) 791.
[12] B.L. Henke, E.M. Gullikson, J.C. Davis, Atom. Data Nucl. Data Table 54 (1993) 181.
[13] C. Riekel, M. Burghammer, G. Schertler, Curr. Opin. Struct. Biol. 15 (2005) 556.
[14] A. McPherson, P. Shlichta, J. Cryst. Growth 90 (1988) 47.
[15] A.K. Singh, A.W. Flounders, J.V. Volponi, C.S. Ashley, K. Wally, J.S. Schoeniger, Biosens. Bioelectron. 14 (1999) 703.
[16] B. Schnyder, R. Kötz, D. Alliata, P. Facci, Surf. Interface Anal. 34 (2002) 40.
[17] M. Birkholz, P. Zaumseil, M. Kittler, I. Wallat, M.P. Heyn, Mater. Sci. Eng. B 134 (2006) 125.
[18] M. Malmsten, in: Y. Lvov, H. Möhwald (Eds.), Protein Architecture, Marcel Dekker, New York, 2000, p. 1.
[19] M. Kittler, X. Yu, O.F. Vyvenko, M. Birkholz, W. Seifert, M. Reiche, T. Wilhelm, T. Arguirov, A. Wolff, W. Fritsche, M. Seibt, Mater. Sci. Eng. C 26 (2006) 902.
[20] M. Birkholz, P. Zaumseil, J. Bauer, D. Bolze, G. Weidner, Mater. Sci. Eng. C 27 (2007) 1154.
[21] E.I. Givargizov, M.O. Kliya, V.R. Melik-Adamyan, A.I. Grebenko, R.C. DeMattei, R.S. Feigelson, J. Cryst. Growth 112 (1991) 758.
[22] Z. Ren, D. Bourgeois, J.R. Helliwell, K. Moffat, V. Srajer, B.L. Stoddard, J. Synchr. Rad. 6 (1999) 891.
[23] K. Moffat, Crystallography of biological macromolecules, in: M.G. Rossmann, E. Arnold (Eds.), International Tables for Crystallography, vol. F, Kluwer, Dordrecht, 2001, p. 167.
[24] Z.H. Kalman, Acta Crystallogr. A 35 (1979) 634.
[25] M. Birkholz, *GILaue* (MatLab program), available from the author on request, 2007.
[26] M. Birkholz, I. Zizak, N. Darowski, I. Wallat, H. Otto, M.P. Heyn, BESSY Annual Report, 2008.